ACS central science

Research Article

Cite This: ACS Cent. Sci. 2019, 5, 458−467

http://pubs.acs.org/journal/acscii

A Bioinspired Scaffold with Anti-Inflammatory Magnesium Hydroxide and Decellularized Extracellular Matrix for Renal Tissue Regeneration

Eugene Lih,[†,▽] Wooram Park,[‡,▽] Ki Wan Park,[†,§] So Young Chun,[∥] Hyuncheol Kim,[§] Yoon Ki Joung,[†] Tae Gyun Kwon,[⊥] Jeffrey A. Hubbell,[*,#] and Dong Keun Han[*,‡]

[†]Center for Biomaterials, Korea Institute of Science and Technology, Seoul 02792, Republic of Korea

[‡]Department of Biomedical Science, College of Life Sciences, CHA University, 335 Pangyo-ro, Bundang-gu, Seongnam, Gyeonggi 13488, Republic of Korea

[§]Department of Chemical and Biomolecular Engineering, Sogang University, Seoul 04107, Republic of Korea

[∥]BioMedical Research Institute, Kyungpook National University Hospital, Daegu 41944, Republic of Korea

[⊥]Department of Urology, School of Medicine, Kyungpook National University, Daegu 37224, Republic of Korea

[#]Institute for Molecular Engineering, University of Chicago, Chicago, Illinois 60637, United States

Supporting Information

ABSTRACT: Kidney diseases are a worldwide public health issue. Renal tissue regeneration using functional scaffolds with biomaterials has attracted a great deal of attention due to limited donor organ availability. Here, we developed a bioinspired scaffold that can efficiently induce renal tissue regeneration. The bioinspired scaffold was designed with poly(lactide-*co*-glycolide) (PLGA), magnesium hydroxide ($Mg(OH)_2$), and decellularized renal extracellular matrix (ECM). The $Mg(OH)_2$ inhibited materials-induced inflammatory reactions by neutralizing the acidic microenvironment formed by degradation products of PLGA, and the acellular ECM helped restore the biological function of kidney tissues. When the PLGA/ECM/$Mg(OH)_2$ scaffold was implanted in a partially nephrectomized mouse model, it led to the regeneration of renal glomerular tissue with a low inflammatory response. Finally, the PLGA/ECM/$Mg(OH)_2$ scaffold was able to restore renal function more effectively than the control groups. These results suggest that the bioinspired scaffold can be used as an advanced scaffold platform for renal disease treatment.

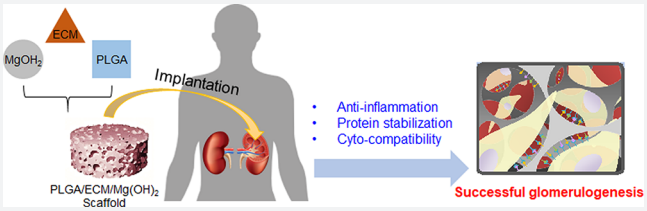

Kidney disease is an international public health problem. In particular, chronic kidney disease (CKD) has been steadily increasing with the prevalence of obesity for the past 30 years.[1,2] Current therapeutic options for CKD are limited to either dialysis or kidney transplantation. Renal transplantation is the optimal treatment for patients suffering from an end-stage renal disease (ESRD) because it improves long-term survival and quality of life.[3] However, limited donor organ availability, graft failure, and numerous complications remain. To address these problems, cell-based therapies using regenerative medicine and tissue engineering have recently been considered for replacing damaged kidney to restore normal kidney function.

To efficiently induce renal tissue regeneration, a scaffolding system is proposed to create an appropriate microenvironment to promote appropriate morphogenesis. The biopolymer, which is the main component of the scaffold, is an important factor because it greatly affects cell growth and function. For decades, biodegradable polyesters have been widely researched and used as a potential material in implantable medical devices for tissue engineering, drug delivery, and invasive surgical treatments due to their desirable characteristics such as easily controlled strength, biodegradability, ease of processability, and the additional avoidable surgery to remove the implants or scaffolds.[4,5] However, there remains a substantial limitation of these biodegradable polymers for some applications, namely, the acidic degradation products of polyesters including poly(lactide-*co*-glycolide) (PLGA). These acidic byproducts decrease the pH of the tissue environment surrounding the implanted polymer, stimulate necrotic cell death, induce inflammatory response and fibrosis,[6−9] and may eventually lead to clinical failure (Figure 1a). Ceonzo et al. and Amini et al. reported that degraded lactic acid and glycolic acid induced a regional inflammatory response following implantation of polyesters due to activation of the complement pathways, resulting in C3a and C5a production and immunoglobulin deposition.[10,11] These anaphylatoxic peptides such as C3a and C5a have been known to increase monocyte and macrophage activity and stimulate macrophages to release proinflammatory

Received: November 6, 2018
Published: January 25, 2019

DOI: 10.1021/acscentsci.8b00812
ACS Cent. Sci. 2019, 5, 458−467

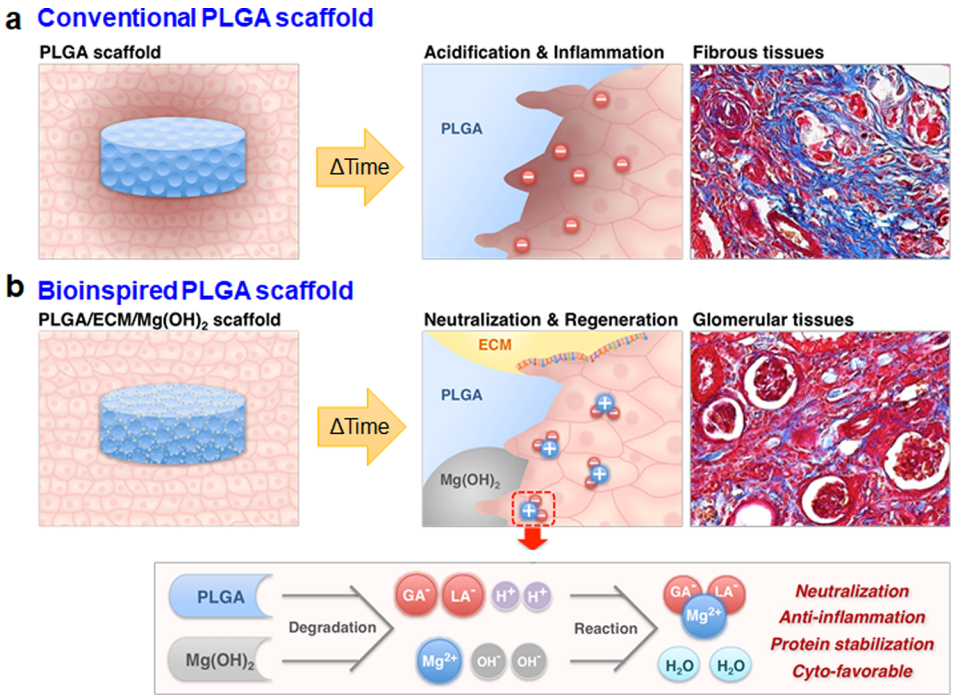

Figure 1. Schematic illustration of a bioinspired scaffold for renal tissue regeneration and its biological and chemical mechanism. Schematic illustration of renal tissue regeneration of (a) conventional and (b) bioinspired PLGA scaffolds. (a) Conventional PLGA scaffold inhibits tissue regeneration due to the inflammatory reaction and fibrosis caused by the acidic microenvironment formed during the degradation process. (b) A bioinspired scaffold neutralizes the acidic microenvironment through the $Mg(OH)_2$ to inhibit the inflammatory response, and have good cytocompatibility by the ECM on a surface of the scaffold. As a result, it efficiently induces glomerularization of kidney cells.

cytokines, such as TNF-α, IL-6, and IL-1β, furthering the foreign body reaction progression.[12,13] Sy et al. also addressed the problem of inflammation in the PLGA-based delivery system whose degradation byproducts caused the activation of p38-regulated signaling pathways in macrophages, and they synthesized a noninflammatory polymer to degrade to neutral and nontoxic products for drug delivery microspheres.[14] In this regard, Wu and co-workers developed polylactide implants coated with a pH-sensitive polymer layer with indomethacin as an anti-inflammatory drug via inhibition of cyclooxygenase; the drug release from the coating layer was faster at a lower pH.[15] The local inflammation resulted from acidosis *in vivo* was suppressed via indomethacin release during the degradation of the polylactide.[15]

Here, we evaluate a magnesium hydroxide ($Mg(OH)_2$) neutralization system within PLGA scaffolds to remedy the major obstacle of PLGA acidification to develop an advanced scaffold platform for renal tissue engineering with histological and functional regeneration. We previously proposed such a $Mg(OH)_2$ neutralization system to suppress PLGA byproduct-induced ensuing cell death and inflammation.[16−18] $Mg(OH)_2$ as a common component of antacids is partially dissolved to produce magnesium and hydroxide ions in water and works by simple neutralization, where the hydroxide ions from $Mg(OH)_2$ combine with acidic H^+ ions.[19] In this regard, $Mg(OH)_2$ particles were utilized to offset the degraded acidic byproducts induced from PLGA, and its neutralization and anti-inflammation effects were demonstrated using various analytic tools. Furthermore, Zhu et al. demonstrated that $Mg(OH)_2$ was successful in retaining the structure and biological activity of encapsulated acid-labile proteins including basic fibroblast growth factor, bovine serum albumin, and bone morphogenetic protein-2 in PLGA matrix by neutralizing the polymer microenvironment pH.[20]

The kidney is a complex organ composed of various cells and complex extracellular matrix (ECM) with proteins, glycosaminoglycans, and growth factors. Since the ECM has components that are appropriate for the growth and function of the kidney cells, acellular renal ECM has been utilized as a supporting material to biologically functionalize PLGA scaffolds.[21] The proteins and growth factors remaining in acellular renal ECM could encourage the reconstruction of glomerulus.[22] Laminins and collagen type IV (Col IV) can, respectively, be involved in the polarization of the developing kidney tubular epithelium and the repair of physiological functions in injured renal proximal tubular cells.[23,24] Moreover, it is well-known that the growth factors such as insulin-like growth factor (IGF), vascular endothelial growth factor (VEGF), epidermal growth factor (EGF), and hepatocyte growth factor (HGF) promote proliferation of renal tubular epithelial cells, recruit endothelial cells in tubulogenesis *in vivo*, and induce mitogenic and morphogenetic responses of renal tubular cells.[25−27]

Here, we designed a bioinspired scaffold with the addition of $Mg(OH)_2$ and acellular ECM to PLGA scaffolds for effective renal regeneration (Figure 1b). $Mg(OH)_2$ could neutralize the acidic microenvironment induced by the acidic decomposed products of PLGA, thereby suppressing undesirable inflammatory reactions. The acellular ECM could promote the normal biological function of kidney cells. Thus, this approach may be used to design advanced functional scaffolds to overcome the disadvantages of conventional PLGA scaffolds and effectively induce regeneration of renal tissue with complex biological functions.

DOI: 10.1021/acscentsci.8b00812
ACS Cent. Sci. 2019, 5, 458−467

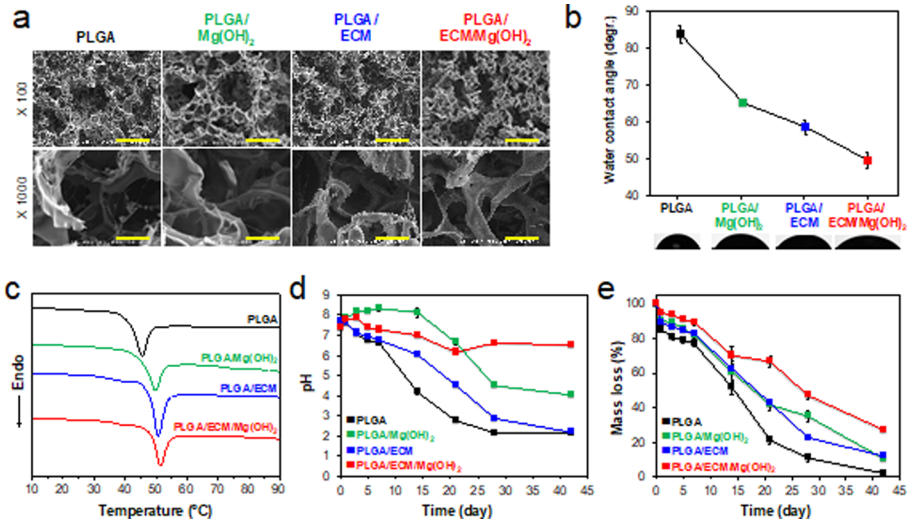

Figure 2. Physicochemical characterization of PLGA/ECM/$Mg(OH)_2$ scaffolds. (a) SEM images of microporous scaffolds (×100, scale bar = 300 μm; and ×1000 magnification, scale bar = 30 μm). (b) Water contact angles and (c) DSC curves of the PLGA-based matrix with $Mg(OH)_2$ and ECM additives. (d) pH changes and (e) mass loss in scaffolds during *in vitro* degradation at 37 °C for 42 days (n = 4).

RESULTS AND DISCUSSION

Bioinspired scaffolds, composed of PLGA, $Mg(OH)_2$, and acellular ECM from porcine kidney (Figure S1, Supporting Information), were fabricated in a cold chamber by an ice particle leaching technique.[21] In the renal tissue regeneration, it is crucial that the implanted scaffold is effectively degraded and replaced by tissue in a short time.[28] Thus, we selected PLGA 50:50 (LA/GA) with fast biodegradation rate.[29] The films with the same components were also prepared by a solvent evaporation method. They are denominated PLGA, PLGA/$Mg(OH)_2$, PLGA/ECM, and PLGA/ECM/$Mg(OH)_2$ scaffolds with the indicated combination of components. Detailed materials and methods for preparation and characterization of the scaffolds are described in the Supporting Information. The existence of $Mg(OH)_2$ and ECM and their proportions in PLGA scaffolds fabricated were verified by measurement of chemico-thermal properties using the attenuated total reflection−Fourier transform infrared (ATR−FTIR, Figure S2, Supporting Information) and thermogravimetric analysis (TGA, Figure S3, Supporting Information). The results from scanning electron microscopy (SEM) showed a highly open-porous and interconnected pore structure that was favorable to nutrient diffusion, cell migration, and metabolic waste removal (Figure 2a). All scaffolds exhibited similar pore size (188 ± 84 μm) and porosity (~90%), regardless of the addition of $Mg(OH)_2$ and ECM, because of the equal ratio of ice particles used to make the scaffolds (Table S1, Supporting Information). The surface wettability of samples was evaluated to confirm the improved hydrophilicity. The dropped water on scaffolds was absorbed within 10 s without PLGA scaffold, and the water contact angle of PLGA matrix decreased from 85° to 48° by adding $Mg(OH)_2$ and ECM (Figure 2b). The hydrophilic property of the scaffold provides certain benefits such as highly efficient cell-seeding and the exchange of culture media in cell-related applications for tissue engineering.[30] Differential scanning calorimetry (DSC) analysis proved that the thermal stability slightly increased when combined with $Mg(OH)_2$ and ECM in the scaffolds, with an increase in melting temperature from 45.5 to 51.4 °C (Figure 2c and Table S1, Supporting Information). Temperature is one of the important parameters affecting the properties of polyesters-based scaffolds, in that degradation is accelerated with proximity to the melting temperature. When the scaffolds that are continuously exposed to body temperature undergo degradation with thermal energy, thermally stable scaffolds (i.e., further from their melting temperature) are more slowly degraded, and also the generation rate of acid byproducts is thus lower. Thus, the slightly increased thermal stability could inhibit local inflammation and cytotoxicity, allowing acidic byproducts to gradually metabolize via the Krebs cycle.[31−33] The mechanical properties of the scaffolds were analyzed by a universal testing machine (UTM). The compressive strength of ECM-containing scaffolds tended to decrease and relatively soften as compared with PLGA scaffold without ECM proteins (Figure S4, Supporting Information).

To assess the neutralizing effect of $Mg(OH)_2$ particles incorporated in PLGA scaffolds, degradation-dependent pH changes (Figure 2d) and mass loss (Figure 2e) of the scaffolds were estimated over 42 days in PBS solution at 37 °C and 100 rpm. During hydrolysis, the pH of all scaffolds changed abruptly for the first 7 days, and the pH changes at the end of the 42 day test period ranged from 2.0 without $Mg(OH)_2$ to 6.5 with neutralization of $Mg(OH)_2$. Although the media with the PLGA/ECM scaffold became acidic as with PLGA, the pH was gradually reduced, probably due to the buffering action of the charged functional groups on ECM according to protein buffer system in which proteins contain histidine that binds to small amounts of acid.[34] The pH buffering capacity of the ECM worked to some advantage to neutralize $Mg(OH)_2$-containing scaffold. In PLGA/$Mg(OH)_2$, the pH increased to 8.5 and then suddenly dropped to 4.5, because the initial burst of $Mg(OH)_2$ in scaffold basified the media and rather accelerated the degradation of PLGA. However, the pH-change behavior of PLGA/ECM/$Mg(OH)_2$ scaffold was relatively flat, which was ascribed the effect of dual neutralization in $Mg(OH)_2$ and ECM components. The pH change and degradation rate depending on $Mg(OH)_2$ were controlled by ECM in the initial phase, and those influenced by the acidic byproducts of PLGA were regulated by $Mg(OH)_2$ as a neutralizing agent afterward. It is thus possible that the gently

DOI: 10.1021/acscentsci.8b00812
ACS Cent. Sci. 2019, 5, 458−467

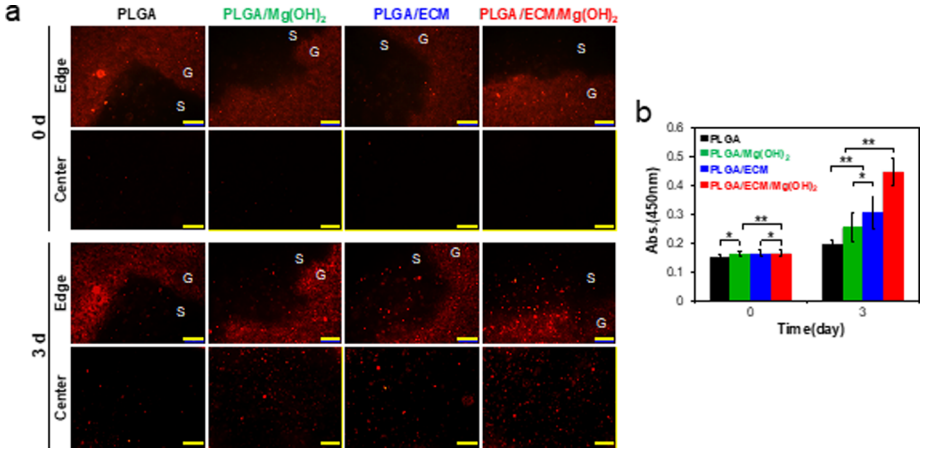

Figure 3. *In vitro* cytocompatibility and cell proliferation on PLGA/ECM/$Mg(OH)_2$ scaffolds. (a) Fluorescence images of HRCEpC labeled with PHK26 around the edges and in the center of scaffolds (S) and collagen gel (G) on the seeding day (0 d) and after 3 days (scale bar = 200 μm). (b) Number of cells in the scaffolds on these days. Values are expressed as mean ± SD (n = 8). *p < 0.05 and **p < 0.005.

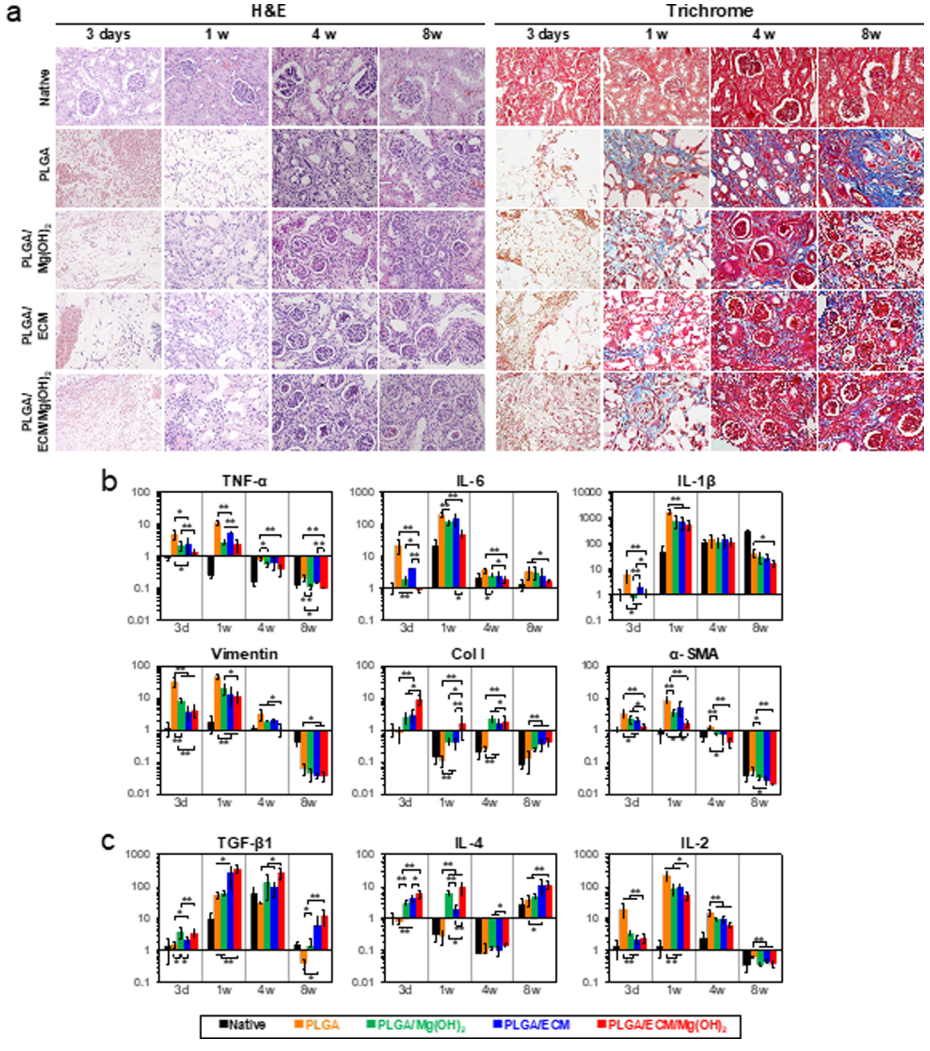

Figure 4. *In vivo* evaluation of renal tissue regeneration capacity and inflammatory response of PLGA/ECM/$Mg(OH)_2$ scaffolds. Reconstruction of PLGA/ECM/$Mg(OH)_2$ scaffolds compared with native renal tissue, PLGA, PLGA/$Mg(OH)_2$, and PLGA/ECM scaffold. (a) H&E and trichrome staining of scaffolds region at 3 days and 1, 4, and 8 weeks (×400 magnification). Gene expression analysis by real-time PCR of (b) proinflammatory markers (tumor necrosis factor alpha, TNF-α; interleukin 6, IL-6; interleukin 1 beta, IL-1β), fibrosis-related markers (vimentin; collagen type I, Col I; alpha-smooth muscle actin, α-SMA), and (c) anti-inflammatory markers (transforming growth factor beta 1, TGF-β1; interleukin 4, IL-4; interleukin 2, IL-2) by real-time PCR. Values are expressed as mean ± SD (n = 6). *p < 0.05 and **p < 0.005.

DOI: 10.1021/acscentsci.8b00812
ACS Cent. Sci. 2019, 5, 458−467

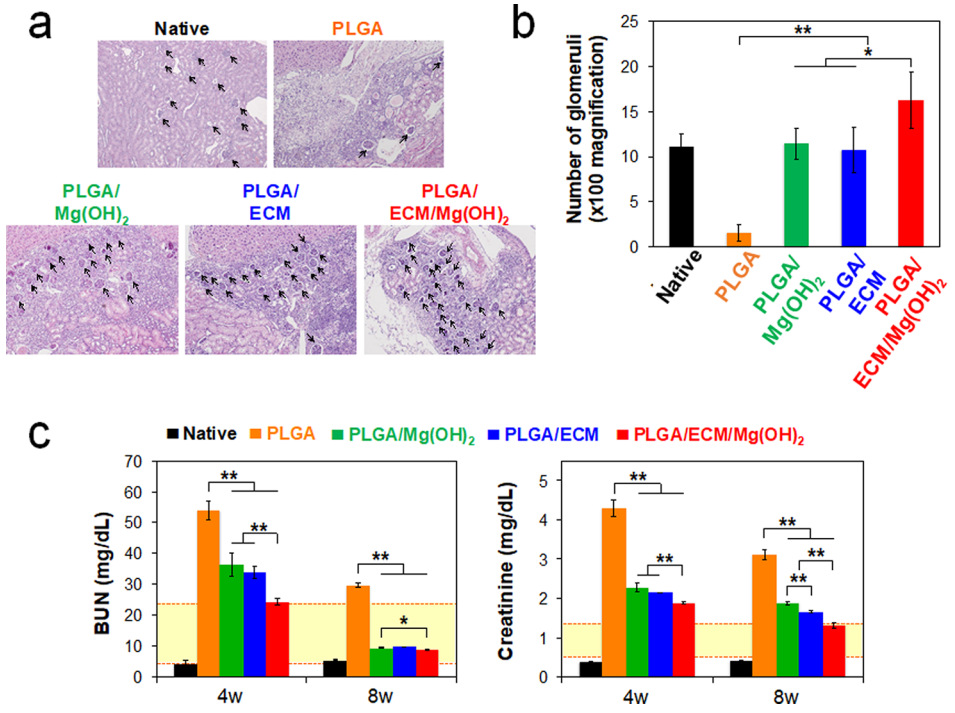

Figure 5. *In vivo* evaluation of renal function recovery of PLGA/ECM/$Mg(OH)_2$ scaffolds. (a) Representative H&E staining of implanted scaffolds for assessment of regenerated glomeruli at 4 weeks postimplantation (black arrows indicate the regenerated glomeruli, ×100 magnification). (b) Number of regenerated glomeruli per unit area (4860 μm^2) at 4 weeks. Values are expressed as mean ± SD (n = 3). *p < 0.01 and **p < 0.001. PLGA/ECM/$Mg(OH)_2$ scaffold displayed a large number of promotive glomeruli per unit area (16.29 ± 3.15), compared with other groups (native 11.14 ± 1.35; PLGA 1.58 ± 0.98; PLGA/$Mg(OH)_2$ 11.43 ± 1.72; PLGA/ECM 10.71 ± 2.50; respectively). (c) Renal function of the regenerated kidney was evaluated after transplantation of scaffolds at 4 and 8 weeks by measurement of blood urea nitrogen (BUN) and creatinine in the blood (yellow box = normal range).

neutralized and degraded scaffold may allow more physiological cellular activities and provide a desirable environment for tissue regeneration.

Cytocompatibility of and cell proliferation on the scaffolds composed of PLGA, $Mg(OH)_2$, and ECM was evaluated using human renal cortical epithelial cells (HRCEpC). Although the *in vitro* cell-testing environment cannot completely mimic *in vivo* conditions, the *in vitro* cellular results demonstrated that the cytotoxicity of the PLGA scaffold was considerably moderated by just adding $Mg(OH)_2$ to neutralize acidic byproducts as well as addition of ECM to provide bioactive molecules for cell adhesion and growth (Figure S5, Supporting Information). To more certainly confirm the cytocompatibility and bioactivity of PLGA/ECM/$Mg(OH)_2$ scaffold, all empty scaffolds were implanted into HRCEpC-seeded collagen hydrogels in 3D, and then the migration of cells into the scaffolds was investigated. HRCEpC labeled with the fluorophore PKH26 were homogeneously dispersed in collagen gel and almost invisible from the center of all scaffolds to those edges immediately after the implantation of scaffolds into the cell/gel composites (Figure 3a). After 3 days, the cells in collagen gel were spread and proliferated, and cells had migrated into the scaffolds. The inside edge and central part of the PLGA scaffold were just observed with a few cells and were not much different from its initial state. In PLGA/$Mg(OH)_2$ and PLGA/ECM scaffolds, it was apparent that a number of cells smoothly migrated to margins in the middle of scaffolds along those borders and particularly more cells existed within cyto-favorable PLGA/ECM. The PLGA/ECM/$Mg(OH)_2$ scaffold showed significantly increased cell density in both the edge and center as though the cells favorably migrated from the collagen gel to the scaffold. The cells within theses scaffolds were quantitatively analyzed using a cell counting kit, and the result was reflected following the fluorescence imaging data (Figure 3b). *In vitro* cell studies demonstrated that the cytocompatibility of PLGA was improved by utilizing pH-neutralizing $Mg(OH)_2$ and bioactive ECM, and furthermore that the synergistic effect of both components might invest PLGA scaffold with biological activity as well as physicochemical properties to promote cell survival against the toxicity associated with acidic byproducts and to encourage cell functions such as proliferation, adhesion, and migration. The bioactive hybrid system of the PLGA/ECM/$Mg(OH)_2$ scaffold was thus expected to positively influence on cell recruitment and differentiation for the regeneration of damaged tissues.

All scaffolds were implanted into a partially nephrectomized mouse to evaluate scaffold biofunctional capacity and therapeutic potential for the regeneration of injured renal tissue. Erythrocytes were observed amply in all scaffolds on day 3, most notably in PLGA scaffold, and the cells grew into the pores resulting from degradation of the scaffolds within 1 week (Figure 4a). Cells were distributed more tightly in PLGA/$Mg(OH)_2$ and PLGA/ECM than in PLGA, and PLGA/ECM/$Mg(OH)_2$ scaffold showed a relatively high level of ECM secretion with numerous cells. After 4 weeks of transplantation, renal tissues were regenerated, with the migration and proliferation of surrounding cells into areas where the scaffold was decomposed, and newly generated glomeruli were found in all scaffolds except the PLGA control (Figure 5a,b). At 8 weeks, the scaffolds were virtually degraded, and the injured kidney tissues were morphologically and histologically

DOI: 10.1021/acscentsci.8b00812
ACS Cent. Sci. 2019, 5, 458−467

recovered with kidney-related cells in all experimental groups. The PLGA scaffold was filled with sclerosed glomeruli and fibrous connective tissue with multifocal inflammation, whereas PLGA scaffolds containing $Mg(OH)_2$ or ECM components were regenerated more like normal renal tissue with renal corpuscles and distal and proximal convoluted tubules as well as much reduced fibrotic tissues (Figure 4a). The area implanted with PLGA/ECM/$Mg(OH)_2$ scaffold exhibited completely reconstructed kidney tissue not only with large sized and morphologically normal glomeruli but also with distal and proximal convoluted tubules. To confirm the histopathological results, all of the tissue samples were assessed by real-time polymerase chain reaction (PCR) analysis (Figure S7, Supporting Information). Tissues in PLGA scaffolds containing $Mg(OH)_2$ or ECM components showed higher expression levels of mesenchymal and renal-related genes than tissues in PLGA during the implantation period, and the values of tissues within PLGA/ECM/$Mg(OH)_2$ scaffolds were significantly higher than those of all scaffolds.

The inflammatory response resulting from implantation of scaffolds was characterized by IHC and PCR analyses. The expression of inflammatory markers was mainly observed at the group implanted with PLGA scaffold at 3 days, whereas PLGA scaffolds with $Mg(OH)_2$ and ECM that were used either separately or in combination showed relatively faint staining for CD4 T cells, CD8 T cells, dendritic cells, extra domain A of fibronectin (ED-A), and monocyte chemotactic protein 1 (MCP-1) (Figure S8, Supporting Information). The results of proinflammatory and fibrosis-related genes expression showed a more severe inflammatory response to PLGA material for up to 1 week (especially on the third day), allowing a comparison of the statistically significant difference between the alleviation effects of $Mg(OH)_2$ and ECM on the inflammation and concomitant fibrosis (Figure 4b). However, after 4 weeks, it was difficult to distinguish the difference in the inflammatory response to the scaffolds because most of the scaffolds were degraded, and the damaged kidney tissues were restored. On day 3, PLGA/$Mg(OH)_2$ and PLGA/ECM scaffolds generated significantly weaker levels of TNF-α, IL-6, IL-1β, vimentin, Col I, and α-SMA, which is related to inflammation and fibrosis, and were expressed compared to PLGA scaffold. These genes within PLGA/ECM/$Mg(OH)_2$ scaffold were remarkably reduced from about 2.5-fold to over 25-fold compared to those of the PLGA-implanted group. Also noteworthy, the incorporation of $Mg(OH)_2$ to PLGA scaffold efficiently inhibited the inflammatory response, resulting in lower TNF-α, IL-6, and IL-1β expression than the PLGA/ECM.

Thus, this change in histological response occurred from the difference between intrinsic (direct) and extrinsic (indirect) approaches to improving the biocompatibility of PLGA with using $Mg(OH)_2$ and ECM. The pH-neutralizing effect of $Mg(OH)_2$ can countervail intrinsic cytotoxicity resulting from acidic byproducts such as lactic and glycolic acids from the decomposition of PLGA, thereby improving the biocompatibility of PLGA material. The acellular renal ECM containing basement membrane and the mesangial matrix is composed of biologically important proteins (laminin, Col IV, and fibronectin) and containing growth factors (VEGF, IGF, EGF, and HGF) for kidney tissue regeneration.[35] Although these proteins and growth factors are incapable of neutralizing acids, they can confer a biological function on PLGA and enhance its biocompatibility not only through stimulation of cell adhesion, proliferation, and differentiation but also by induction of cell recruitment and migration.[23−27] Hence, $Mg(OH)_2$ directly restricted PLGA-induced inflammation and exhibited lower levels of related genes compared to the ECM-only incorporated scaffold, whereas ECM relatively weakly suppressed the inflammatory response and rather regulated the formation of nonfunctional fibrous tissues in repair tissue. The PLGA/ECM/$Mg(OH)_2$ scaffold could consequently supply an optimal kidney tissue regenerating environment which benefited doubly from pH neutralization and biological functionalization, indicating that the gene expression of proinflammation and fibrosis-related markers was down-regulated. Furthermore, the $Mg(OH)_2$ and ECM contained in the PLGA scaffolds exhibited an anti-inflammatory effect as well as an inflammation-suppressive effect (Figure 4c). The PLGA/ECM/$Mg(OH)_2$ scaffold also showed an increased expression of anti-inflammatory genes such as TGF-b, IL-4, and IL-2 genes. The renal tissue regenerated from bioinspired functional scaffolds had tubular and glomerular structures. Particularly, neovascularity was shown in the PLGA scaffold containing both $Mg(OH)_2$ and renal ECM (Figure S9, Supporting Information). Based on these histological results, such anti-inflammatory and bioactive PLGA/ECM/$Mg(OH)_2$ scaffolds are believed to provide an optimal microenvironment for kidney cells to proliferate and differentiate toward renal lineages.

Recovery of renal function was distinguished by metabolic analysis (Figure 5c). Mice implanted with PLGA scaffolds containing $Mg(OH)_2$ and/or ECM exhibited a rapid amelioration of the renal dysfunction, as evaluated by metabolic markers such as blood urea nitrogen (BUN) and creatinine concentrations. In particular, the significantly better metabolic function was observed in animals treated with the PLGA/ECM/$Mg(OH)_2$ scaffold. At 4 weeks after implantation, BUN levels in animals treated with PLGA/$Mg(OH)_2$ and PLGA/ECM had decreased over 2-fold compared with those treated with PLGA alone (36.4 ± 3.8 and 33.9 ± 2.0 vs 54.0 ± 3.0 mg dL^{-1}), and their creatinine concentrations (2.28 ± 0.11 and 2.15 ± 0.01 mg dL^{-1}) were slightly lower than that of PLGA (4.31 ± 0.21 mg dL^{-1}). However, the metabolic levels of animals treated with PLGA/$Mg(OH)_2$ and PLGA/ECM were not within the normal ranges (BUN 6−23 mg dL^{-1} and creatinine 0.7−1.3 mg dL^{-1}),[36,37] and neither were those of animals treated with the PLGA control scaffold. However, consistent with our expectation, the mice implanted with PLGA/ECM/$Mg(OH)_2$ scaffold had a larger normalization of their metabolic levels at 4 weeks postoperation than other groups, which were approaching normal levels: BUN 23.3 ± 0.8 mg dL^{-1} and creatinine 1.89 ± 0.02 mg dL^{-1}, respectively. It was thus demonstrated that the PLGA/ECM/$Mg(OH)_2$ scaffold helped the injured kidney of mice recovered much faster with biocompatible and biofunctional support attributed to the synergistic effect of $Mg(OH)_2$ and renal ECM, as contrasted with the response in mice treated with the other control scaffolds. At the longer time point of 8 weeks, mice implanted with PLGA/$Mg(OH)_2$, PLGA/ECM, or PLGA/ECM/$Mg(OH)_2$ scaffolds demonstrated a steady decrease of BUN and creatinine levels, but a lack of functional recovery was observed in PLGA scaffold control. Only the mice treated with the PLGA/ECM/$Mg(OH)_2$ scaffold demonstrated values in the normal range of creatinine levels at 8 weeks. When an indigo carmine solution was injected into the blood vessels to determine the number of glomeruli that exerted normal renal function, a functionally regenerated number of glomeruli

DOI: 10.1021/acscentsci.8b00812
ACS Cent. Sci. 2019, 5, 458−467

similar to the native was shown in PLGA/ECM/$Mg(OH)_2$ group (Figure S6, Supporting Information). These results imply that the successful regeneration of the structure and function of kidney tissue in the functional scaffold is due to the interaction of cells with bioactive molecules on the decellularized ECM. In addition, the inhibition of inflammatory responses by $Mg(OH)_2$ during decomposition of polyester could also support the renal regeneration.

CONCLUSIONS

The number of patients with chronic kidney disease is rising worldwide,[38] but the treatment is still dependent on dialysis and kidney transplantation. These therapies have some drawbacks such as high cost, the risk of immune rejection, and lack of donor organ availability, motivating many researchers to pursue tissue engineering techniques as an alternative therapy using biodegradable scaffolds to adequately support cell proliferation and differentiation.[39−42] However, further engineering of PLGA, which has been used as a biomaterial for the biodegradable scaffold, is required to improve its biocompatibility because the harmful acidic degradation of PLGA may cause inflammation and hinder functional recovery of tissues.[43,44] Our data suggest that supplementing the antacid $Mg(OH)_2$ and bioactive acellular renal ECM in the polymeric scaffold alleviated the inflammatory response and activated cell morphogenetic behaviors, influencing cell attachment and differentiation and exchange of metabolites. Moreover, the PLGA/ECM/$Mg(OH)_2$ scaffold promoted the reconstruction of glomerular structure and tubules in renal tissues and contributed to the full functional recovery of the partially nephrectomized kidney. Our study focused on the synergistic effect of an acid-neutralizing agent and bioactive molecules on anti-inflammation and biofunctionality of biodegradable polyester-based medical implants. This versatile system not only may apply to a new treatment strategy of chronic kidney disease as explored herein, but may also be useful for the development of advanced biomedical devices consisting of an implant, graft, or stents based on degradable polyesters.

MATERIALS AND METHODS

Materials. Magnesium hydroxide ($Mg(OH)_2$) was purchased from Junsei Chemical Co. (Tokyo, Japan). Poly(D,L-lactide-*co*-glycolide) (PLGA, LA:GA = 50:50, MW 40 000) was obtained from Evonik Ind. (Essen, Germany). PKH26 red fluorescent cell linker kit, dichloromethane (DCM), deoxyribonuclease (DNase), and collagenase (125 units mg^{-1}) were purchased from Sigma-Aldrich Co. (St. Louis, MO). Renal epithelial cell growth kit, human renal cortical epithelial cells (HRCEpC), and renal epithelial cell basal medium were obtained from the American Type Culture Collection (ATCC, Manassas, VA). The 4′,6-diamidino-2-phenylindole (DAPI), streptomycin, penicillin, hematoxylin and eosin (H&E), Triton X-100, trichrome stain kit, and phosphate-buffered saline (PBS) solution were purchased from Invitrogen (Rockville, MD). Collagen type I (from rat tail tendons, 4 mg mL^{-1}) was purchased form R&D systems (Minneapolis, MN). Indigo carmine was obtained from Akorn Inc. (Buffalo Grove, IL). Cell Counting Kit-8 (CCK-8) assay was obtained from Dojindo Molecular Technology (Tokyo, Japan).

Preparation of Acellular Renal ECM. The ECM powder was prepared by decellularization of the porcine kidney (Cortical sections ($10 \times 10 \times 2$ mm^3), Yorkshire pigs, female, 2−3 months, 22−30 kg) according to the conventional method.[35] Briefly, porcine kidney tissues were washed several times with PBS and incubated in a decellularizing solution at 4 °C, 200 rpm for 14 days. The decellularizing solution was prepared with Triton X-100 1% (v/v) including streptomycin (100 ug mL^{-1}) and penicillin (100 U mL^{-1}). After the decellularization process, tissues were washed with PBS and incubated in PBS containing DNase (30 μg mL^{-1}) for 1 h. The decellularized kidney tissues were again washed several times with PBS and lyophilized for 3 days. H&E and DAPI staining were performed to confirm that the ECM was completely decellularized. The ECM from porcine kidney tissues was freeze-milled with a Freezer/Mill 6750 instrument from SPEX CertiPrep (Metuchen, NJ) and sterilized with ethylene oxide (EO) gas (PERSON-EO35 sterilizer, Person Medical Co., Gunpo, Korea) for further experiments (Figure S1, Supporting Information).

Fabrication of $Mg(OH)_2$ and ECM Incorporated PLGA Scaffolds and Films. The PLGA scaffolds with $Mg(OH)_2$ and ECM components were fabricated using ice microparticles as a porogen, as previously reported.[17,21] In the manufacturing process, PLGA was dissolved with 15 wt % in DCM, and $Mg(OH)_2$ and ECM were incorporated at 15 and 10 wt % of the PLGA mass, respectively. The prepared scaffolds are named as PLGA, PLGA/$Mg(OH)_2$, PLGA/ECM, and PLGA/ECM/$Mg(OH)_2$ with the following type of components. As a control group, the group containing only PLGA was used. The manufacturing method was as described above except that it contained only PLGA. Film-shaped samples were also prepared with the above composition, as previously reported.[21] Until the experiments, all samples were stored at −20 °C.

Characterizations of PLGA/ECM/$Mg(OH)_2$ Matrix. The morphology of the prepared scaffolds was analyzed by scanning electron microscopy (FE-SEM; Hitachi S-4800). The porosity of the scaffold was measured by analyzing randomly selected SEM images with ImageJ software (National Institutes of Health), as previously reported.[21,45] The ATR−FTIR (4100, JASCO, MD) analysis was performed to study the molecular conformation of the scaffold as following our previous report.[21] The TGA (TA Instruments Hi-Res TGA 2950) was performed to measure the mass of $Mg(OH)_2$ and ECM contained in the scaffold. The detailed analysis procedure for the TGA was the same as that previously reported.[21] The prepared scaffolds were analyzed with differential scanning calorimetry (DSC; DSC-Q20, TA Instruments) to determine the thermal stability of scaffolds. The detailed DSC analysis was performed according to that previously reported.[21] The prepared scaffolds were analyzed with a UTM (Instron 4464, Norwood, MA) to determine the mechanical compressive properties. The detailed UTM measurement was performed according to that previously reported.[21] To measure the hydrophilicity/hydrophobicity of the surface of the scaffolds, the water contact angle (WCA) was determined with contact angle goniometry (VCA Optima XE Video Contact Angle System, Crest Technology, Singapore) at room temperature, as previously reported.[21] To evaluate neutralizing and buffering effects of $Mg(OH)_2$ and ECM on the degradation of PLGA, pH changes and mass loss were measured. Each sample was individually immersed in 10 mL of PBS in a glass vial and dynamically incubated at 37 °C with 100 rpm. At every defined time interval, the pH of media was assessed by pH meter (Orion, Thermo electron co.), and then samples were rinsed with distilled water and lyophilized

DOI: 10.1021/acscentsci.8b00812
ACS Cent. Sci. 2019, 5, 458−467

for 4 days. The percentage mass loss was calculated with the following equation: mass loss (%) = $(mass_i - mass_d)/mass_i \times 100$, where $mass_i$ is the initial mass of the sample, and $mass_d$ is the mass of the dried sample.

***In Vitro* Cell Study.** We used HRCEpC cells to assess the biocompatibility of the prepared scaffolds. HRCEpC cells were cultured under the same conditions as our previous study.[21] To evaluate the cytocompatibility of the prepared PLGA/Mg-$(OH)_2$/ECM film, HRCEpC cells (2×10^5 cells mL^{-1}) were cultured on the films (1×1 cm^2) in 24-well plates, and the CCK-8 assay was performed at a predetermined time (1, 3, and 5 days). The absorbance of the CCK-8 was measured at 450 nm using a microplate reader (Multiskan Spectrum, Thermo Electron Co., Vantaa, Finland). To assess the biological affinity and activity of the scaffolds, the cellular migration test was performed in cell-containing collagen gels. HRCEpC were labeled with the fluorescent PKH26 at the end of the isolated by the manufacturing protocol. Briefly, after trypsin release and washing, cells were suspended in 1 mL of diluent and mixed with the same volume of the labeling solution containing PKH26 in diluent to the final concentration of 4 μM. After 5 min of incubation in the dark, the labeling reaction was stopped by adding 2 mL of fetal bovine serum (FBS), and the cells were washed three times in complete medium before use. Collagen solution (1.5 mg mL^{-1}) was prepared with labeled cells at a concentration of 5×10^6 cells mL^{-1}, and 150 μL of the cell-loaded collagen solution was placed in each well of the nontreated 96-well plate. The well plate was incubated to polymerize collagen for 15 min at 37 °C and 5% CO_2. Before fully gelling, the cell-free scaffolds ($2 \times 2 \times 2$ mm^3) that were hydrated with PBS and warmed to 37 °C were carefully implanted into the core of the collagen matrix. The mixtures of scaffolds and collagen/cell matrix were completely polymerized with additional incubation under the above-mentioned conditions for 30 min, and then 100 μL of complete medium was added to each well. After 4 h (0 day) and 3 days, the cells in the plate were visualized using a fluorescence microscopy for observation of cell movement within these mixtures. To quantitatively analyze the migrated cells from collagen gel into scaffolds, the scaffolds were pulled from the collagen/cell matrix at different time points (0 and 3 days). These scaffolds were treated with collagenase (1 mg mL^{-1}) at 37 °C and 5% CO_2 for 10 min and gently rinsed three times with complete medium to ensure full dissociation of the scaffolds without adhered residual collagen/cell outside scaffolds. The samples were transferred to a new 96-well plate and evaluated by the CCK-8 assay.

***In Vivo* Model Design.** For *in vivo* study, 5 week old, male ICR mice (20 g) (Orient Bio Inc., Seongnam, Korea) were randomized into five groups; native control, PLGA, PLGA/$Mg(OH)_2$, PLGA/ECM, and PLGA/ECM/$Mg(OH)_2$ scaffolds (each group $n = 30$). The left kidney has exposed the back through a surgical operation, and partial nephrectomy (excision volume, $5 \times 2 \times 2$ mm^3) was performed to evaluate renal tissue regeneration ability of the scaffolds. The scaffolds were implanted into the defected site. The right kidney was completely removed to confirm the effects of tissue regeneration by the scaffold. The operated mice were sacrificed at 3 days and 1, 4, and 8 weeks after the operation, and their kidneys were retrieved for subsequent histology, immunohistochemistry, and gene expression analysis (6 mice per period from each group). Scaffolds and tissues extracted from animals were classified for further histology and real-time PCR analysis. All procedures were performed by an animal protocol approved by Yeungnam University Hospital Institutional Animal Care and Use Committee (YUMC-AEC2016-003).

Histological and Functional Analyses. Histological analysis was performed by an expert pathologist including inflammatory and immune-related cell infiltration, renal progenitor cell migration, regenerated glomerular morphology assessment, and renal tubule regeneration. The histological and immunohistochemical (IHC) analyses were performed by the previously reported method.[21] Half of each extracted tissues were used for real-time PCR analysis. In the real-time PCR analysis, the $2^{-\Delta\Delta Ct}$ method was utilized to analyze relative gene expression changes. To evaluate renal function, blood urea nitrogen (BUN) and urinary creatinine levels were measured by external entrustment (Samkwang Medical Lab., Seoul, Korea). Also, indigo carmine staining was performed to confirm the filtration of the regenerated renal glomeruli.[46] The original solution of indigo carmine (30 μL) was injected into the renal artery, and then the kidneys were collected and cryosectioned with a thickness of 50 μm. All the tissue sections were observed by optical microscopy (Olympus).

Statistical Analysis. All experimental results were obtained through more than three iterations, and the values were described as mean ± standard deviations. The statistical significance was analyzed by Student t test. The statistically significant difference was defined as the p value being less than 0.05.

Safety Statement. No unexpected or unusually high safety hazards were encountered in this line of research.

■ ASSOCIATED CONTENT

Supporting Information

The Supporting Information is available free of charge on the ACS Publications website at DOI: 10.1021/acscentsci.8b00812.

Physical characteristic data for the prepared scaffolds; and histology and real-time PCR data for PLGA/ECM/$Mg(OH)_2$ scaffold (PDF)

■ AUTHOR INFORMATION

Corresponding Authors

*E-mail: jhubbell@uchicago.edu.
*E-mail: dkhan@cha.ac.kr.

ORCID

Wooram Park: 0000-0002-4614-0530
Yoon Ki Joung: 0000-0001-8661-481X
Jeffrey A. Hubbell: 0000-0003-0276-5456
Dong Keun Han: 0000-0002-3852-3160

Author Contributions

[▽]E.L. and W.P. equally contributed to this work. The manuscript was written through the contributions of all authors. All authors have approved the final version of the manuscript.

Notes

The authors declare no competing financial interest.

■ ACKNOWLEDGMENTS

This work was supported by Basic Science Research Program (2017R1A2B3011121) and Bio & Medical Technology Development Programs (2014M3A9D3033887 and 2018M3A9E2024579) through the National Research Foun-

DOI: 10.1021/acscentsci.8b00812
ACS Cent. Sci. 2019, 5, 458−467

dation of Korea funded by the Ministry of Science and ICT (MSIT) and a grant of the Korea Health Technology R&D Project (HI18C0089) through the Korea Health Industry Development Institute (KHIDI), funded by the Ministry of Health & Welfare, Republic of Korea.

REFERENCES

(1) Levey, A.; Atkins, R.; Coresh, J.; Cohen, E.; Collins, A.; Eckardt, K.-U.; Nahas, M.; Jaber, B.; Jadoul, M.; Levin, A. Chronic kidney disease as a global public health problem: approaches and initiatives—a position statement from Kidney Disease Improving Global Outcomes. *Kidney Int.* **2007**, *72* (3), 247.

(2) Schieppati, A.; Remuzzi, G. Chronic renal diseases as a public health problem: epidemiology, social, and economic implications. *Kidney Int.* **2005**, *68*, S7.

(3) Uzarski, J. S.; Xia, Y.; Belmonte, J. C.; Wertheim, J. A. New strategies in kidney regeneration and tissue engineering. *Curr. Opin. Nephrol. Hypertens.* **2014**, *23* (4), 399.

(4) Grafahrend, D.; Heffels, K.-H.; Beer, M. V.; Gasteier, P.; Möller, M.; Boehm, G.; Dalton, P. D.; Groll, J. Degradable polyester scaffolds with controlled surface chemistry combining minimal protein adsorption with specific bioactivation. *Nat. Mater.* **2011**, *10* (1), 67.

(5) Do, A. V.; Khorsand, B.; Geary, S. M.; Salem, A. K. 3D printing of scaffolds for tissue regeneration applications. *Adv. Healthcare Mater.* **2015**, *4* (12), 1742.

(6) Houchin, M.; Topp, E. Chemical degradation of peptides and proteins in PLGA: a review of reactions and mechanisms. *J. Pharm. Sci.* **2008**, *97* (7), 2395.

(7) Kapoor, D. N.; Bhatia, A.; Kaur, R.; Sharma, R.; Kaur, G.; Dhawan, S. PLGA: a unique polymer for drug delivery. *Ther. Delivery* **2015**, *6* (1), 41.

(8) Kim, M. S.; Ahn, H. H.; Shin, Y. N.; Cho, M. H.; Khang, G.; Lee, H. B. An *in vivo* study of the host tissue response to subcutaneous implantation of PLGA-and/or porcine small intestinal submucosa-based scaffolds. *Biomaterials* **2007**, *28* (34), 5137.

(9) Martins, C.; Sousa, F.; Araújo, F.; Sarmento, B. Functionalizing PLGA and PLGA derivatives for drug delivery and tissue regeneration applications. *Adv. Healthcare Mater.* **2018**, *7* (1), 1701035.

(10) Ceonzo, K.; Gaynor, A.; Shaffer, L.; Kojima, K.; Vacanti, C. A.; Stahl, G. L. Polyglycolic acid-induced inflammation: role of hydrolysis and resulting complement activation. *Tissue Eng.* **2006**, *12* (2), 301.

(11) Amini, A. R.; Wallace, J. S.; Nukavarapu, S. P. Short-term and long-term effects of orthopedic biodegradable implants. *J. Long-Term Eff. Med. Implants* **2011**, *21* (2), 93.

(12) Luttikhuizen, D. T.; van Amerongen, M. J.; de Feijter, P. C.; Petersen, A. H.; Harmsen, M. C.; van Luyn, M. J. The correlation between difference in foreign body reaction between implant locations and cytokine and MMP expression. *Biomaterials* **2006**, *27* (34), 5763.

(13) Nilsson, B.; Ekdahl, K. N.; Mollnes, T. E.; Lambris, J. D. The role of complement in biomaterial-induced inflammation. *Mol. Immunol.* **2007**, *44* (1), 82.

(14) Sy, J. C.; Seshadri, G.; Yang, S. C.; Brown, M.; Oh, T.; Dikalov, S.; Murthy, N.; Davis, M. E. Sustained release of a p38-inhibitor from non-inflammatory microspheres inhibits cardiac dysfunction. *Nat. Mater.* **2008**, *7* (11), 863.

(15) Wu, D.; Chen, X.; Chen, T.; Ding, C.; Wu, W.; Li, J. Substrate-anchored and degradation-sensitive anti-inflammatory coatings for implant materials. *Sci. Rep.* **2015**, *5*, 11105.

(16) Kum, C. H.; Cho, Y.; Joung, Y. K.; Choi, J.; Park, K.; Seo, S. H.; Park, Y. S.; Ahn, D. J.; Han, D. K. Biodegradable poly(l-lactide) composites by oligolactide-grafted magnesium hydroxide for mechanical reinforcement and reduced inflammation. *J. Mater. Chem. B* **2013**, *1* (21), 2764.

(17) Lee, H. W.; Seo, S. H.; Kum, C. H.; Park, B. J.; Joung, Y. K.; Son, T. I.; Han, D. K. Fabrication and characteristics of anti-inflammatory magnesium hydroxide incorporated PLGA scaffolds formed with various porogen materials. *Macromol. Res.* **2014**, *22* (2), 210.

(18) Lih, E.; Kum, C. H.; Park, W.; Chun, S. Y.; Cho, Y.; Joung, Y. K.; Park, K.-S.; Hong, Y. J.; Ahn, D. J.; Kim, B.-S.; Kwon, T. G.; Jeong, M. H.; Hubbell, A. H.; Han, D. K. Modified Magnesium Hydroxide Nanoparticles Inhibits the Inflammatory Response to Biodegradable Poly(lactide-co-glycolide)(PLGA) Implants. *ACS Nano* **2018**, *12* (7), 6917.

(19) Lin, M.-S.; Sun, P.; Yu, H.-Y. Evaluation of buffering capacity and acid neutralizing-pH time profile of antacids. *J. Formos. Med. Assoc.* **1998**, *97* (10), 704—710.

(20) Zhu, G.; Mallery, S. R.; Schwendeman, S. P. Stabilization of proteins encapsulated in injectable poly(lactide-co-glycolide). *Nat. Biotechnol.* **2000**, *18* (1), 52.

(21) Lih, E.; Park, K. W.; Chun, S. Y.; Kim, H.; Kwon, T. G.; Joung, Y. K.; Han, D. K. Biomimetic porous PLGA scaffolds incorporating decellularized extracellular matrix for kidney tissue regeneration. *ACS Appl. Mater. Interfaces* **2016**, *8* (33), 21145.

(22) Yu, Y.; Shao, Y.; Ding, Y.; Lin, K.; Chen, B.; Zhang, H.; Zhao, L.; Wang, Z.; Zhang, J.; Tang, M. Decellularized kidney scaffold-mediated renal regeneration. *Biomaterials* **2014**, *35* (25), 6822.

(23) Mak, G. Z.; Kavanaugh, G. M.; Buschmann, M. M.; Stickley, S. M.; Koch, M.; Goss, K. H.; Waechter, H.; Zuk, A.; Matlin, K. S. Regulated synthesis and functions of laminin 5 in polarized Madin-Darby canine kidney epithelial cells. *Mol. Biol. Cell* **2006**, *17* (8), 3664.

(24) Nony, P. A.; Schnellmann, R. G. Mechanisms of renal cell repair and regeneration after acute renal failure. *J. Pharmacol. Exp. Ther.* **2002**, *304* (3), 905.

(25) Villegas, G.; Lange-Sperandio, B.; Tufro, A. Autocrine and paracrine functions of vascular endothelial growth factor (VEGF) in renal tubular epithelial cells. *Kidney Int.* **2005**, *67* (2), 449.

(26) Neuss, S.; Becher, E.; Wöltje, M.; Tietze, L.; Jahnen-Dechent, W. Functional expression of HGF and HGF receptor/c-met in adult human mesenchymal stem cells suggests a role in cell mobilization, tissue repair, and wound healing. *Stem Cells* **2004**, *22* (3), 405.

(27) Vargas, G. A.; Hoeflich, A.; Jehle, P. M. Hepatocyte growth factor in renal failure: promise and reality. *Kidney Int.* **2000**, *57* (4), 1426.

(28) O'brien, F. J. Biomaterials & scaffolds for tissue engineering. *Mater. Today* **2011**, *14* (3), 88.

(29) Farahani, T. D.; Entezami, A. A.; Mobedi, H.; Abtahi, M. Degradation of poly(D,L-lactide-co-glycolide) 50:50 implant in aqueous medium. *Iran Polym. J.* **2005**, *14* (8), 753.

(30) Bhattarai, S. R.; Bhattarai, N.; Viswanathamurthi, P.; Yi, H. K.; Hwang, P. H.; Kim, H. Y. Hydrophilic nanofibrous structure of polylactide; fabrication and cell affinity. *J. Biomed. Mater. Res., Part A* **2006**, *78* (2), 247.

(31) Wang, Z.; Wang, Y.; Ito, Y.; Zhang, P.; Chen, X. A comparative study on the *in vivo* degradation of poly(L-lactide) based composite implants for bone fracture fixation. *Sci. Rep.* **2016**, *6*, 20770.

(32) Liu, Y.; Bai, X.; Liang, A. Synthesis, properties, and *in vitro* hydrolytic degradation of poly(d,l-lactide-co-glycolide-co-ε-caprolactone). *Int. J. Polym. Sci.* **2016**, *2016*, 80820114.

(33) Shive, M. S.; Anderson, J. M. Biodegradation and biocompatibility of PLA and PLGA microspheres. *Adv. Drug Delivery Rev.* **1997**, *28* (1), 5.

(34) Theocharis, A. D.; Skandalis, S. S.; Gialeli, C.; Karamanos, N. K. Extracellular matrix structure. *Adv. Drug Delivery Rev.* **2016**, *97*, 4.

(35) Choi, S. H.; Chun, S. Y.; Chae, S. Y.; Kim, J. R.; Oh, S. H.; Chung, S. K.; Lee, J. H.; Song, P. H.; Choi, G. S.; Kim, T. H. Development of a porcine renal extracellular matrix scaffold as a platform for kidney regeneration. *J. Biomed. Mater. Res., Part A* **2015**, *103* (4), 1391.

(36) Stender, R. N.; Engler, W. J.; Braun, T. M.; Hankenson, F. C. Establishment of blood analyte intervals for laboratory mice and rats by use of a portable clinical analyzer. *J. Am. Assoc. Lab. Anim. Sci.* **2007**, *46* (3), 47—52.

DOI: 10.1021/acscentsci.8b00812
ACS Cent. Sci. 2019, 5, 458—467

(37) Yuen, P. S.; Dunn, S. R.; Miyaji, T.; Yasuda, H.; Sharma, K.; Star, R. A. A simplified method for HPLC determination of creatinine in mouse serum. *Am. J. Physiol. Renal Physiol.* **2004**, *286* (6), F1116.
(38) Liyanage, T.; Ninomiya, T.; Jha, V.; Neal, B.; Patrice, H. M.; Okpechi, I.; Zhao, M.-h.; Lv, J.; Garg, A. X.; Knight, J. Worldwide access to treatment for end-stage kidney disease: a systematic review. *Lancet* **2015**, *385* (9981), 1975.
(39) Wang, X.; Shan, H.; Wang, J.; Hou, Y.; Ding, J.; Chen, Q.; Guan, J.; Wang, C.; Chen, X. Characterization of nanostructured ureteral stent with gradient degradation in a porcine model. *Int. J. Nanomed.* **2015**, *10*, 3055.
(40) Maeda, N.; Verret, V.; Moine, L.; Bédouet, L.; Louguet, S.; Servais, E.; Osuga, K.; Tomiyama, N.; Wassef, M.; Laurent, A. Targeting and recanalization after embolization with calibrated resorbable microspheres versus hand-cut gelatin sponge particles in a porcine kidney model. *J. Vasc. Interv. Radiol.* **2013**, *24* (9), 1391.
(41) Basu, J.; Genheimer, C. W.; Rivera, E. A.; Payne, R.; Mihalko, K.; Guthrie, K.; Bruce, A. T.; Robbins, N.; McCoy, D.; Sangha, N. Functional evaluation of primary renal cell/biomaterial Neo-Kidney Augment prototypes for renal tissue engineering. *Cell Transplant* **2011**, *20* (11−12), 1771.
(42) Roessger, A.; Denk, L.; Minuth, W. W. Potential of stem/progenitor cell cultures within polyester fleeces to regenerate renal tubules. *Biomaterials* **2009**, *30* (22), 3723.
(43) Yoon, S. J.; Kim, S. H.; Ha, H. J.; Ko, Y. K.; So, J. W.; Kim, M. S.; Yang, Y. I.; Khang, G.; Rhee, J. M.; Lee, H. B. Reduction of Inflammatory Reaction of Poly(D,L-Lactic-co-Glycolic Acid) Using Demineralized Bone Particles. *Tissue Eng., Part A* **2008**, *14* (4), 539.
(44) Lendlein, A.; Langer, R. Biodegradable, elastic shape-memory polymers for potential biomedical applications. *Science* **2002**, *296* (5573), 1673.
(45) Fouad, H.; Elsarnagawy, T.; Almajhdi, F. N.; Khalil, K. A. Preparation and *in vitro* thermo-mechanical characterization of electrospun PLGA nanofibers for soft and hard tissue replacement. *Int. J. Electrochem. Sci.* **2013**, *8*, 2293.
(46) Snyder, K.; Keegan, C. *Pharmacology for the surgical technologist*; Elsevier Health Sciences, 2016.

DOI: 10.1021/acscentsci.8b00812
ACS Cent. Sci. 2019, 5, 458−467